Supplementary Information

Interfacial Passivation of Wide-bandgap Perovskite Solar Cells and Tandem Solar Cells

Rui Xia[a,†], Yibo Xu[b,†], Bingbing Chen[c,†], Hiroyuki Kanda[d], Marius Franckevičius[e], Rokas Gegevičius[e], Shubo Wang[b], Yifeng Chen[a], Daming Chen[a], Jianning Ding[b], Ningyi Yuan[b,*], Ying Zhao[c], Cristina Roldán-Carmona[d*], Xiaodan Zhang[c,*], Paul J. Dyson[f], Mohammad Khaja Nazeeruddin[d,*]

a. State Key Lab of Photovoltaic Science and Technology, Trina Solar, ChangZhou, 213031, China

b. School of Materials Science and Engineering; Jiangsu Collaborative Innovation Center for Photovoltaic Science and Engineering; Jiangsu Province Cultivation base for State Key Laboratory of Photovoltaic Science and Technology, Changzhou University, Changzhou, 213164, China. nyyuan@cczu.edu.cn

c. Institute of Photoelectronic Thin Film Devices and Technology of Nankai University, Tianjin 300071, China. xdzhang@nankai.edu.cn

d. Group for Molecular Engineering of Functional Materials Institute of Chemical Sciences and Engineering, École Polytechnique Fédérale de Lausanne (EPFL), Sion, CH-1951, Switzerland. Cristina.roldancarmona@epfl.ch; mdkhaja.nazeeruddin@epfl.ch

e. Center for Physical Sciences and Technology, Savanoriu̧ Ave. 231, LT‐02300 Vilnius, Lithuania.

f. Institut des Sciences et Ingénierie Chimiques, Ecole Polytechnique Fédérale de Lausanne (EPFL), CH‐1015 Lausanne, Switzerland.

Experimental Section

Materials: PbI_2 (>99%), $PbBr_2$ (>99%), FAI (Formamidinium iodide, >99%), and CsI (>99%) were purchased from Xi'an Polymer Light Technology. N, N-dimethylformamide (DMF, >99.9%), dimethyl sulfoxide (DMSO, >99.9%), and $NbCl_5$ (99.9%) were obtained from Alfa Aesar. Spiro-OMeTAD was purchased from Borun New Material Technology. $TiCl_4$ (99.9%) was purchased from Aladdin. All the materials were directly used without further purification. Fluorine-doped tin oxide on glass (FTO glass, square resistance: 6-8 ohm/sq, Haze: 11-17%) was obtained from Asahi Glass Co., LTD (AGC).

Fabrication of single-junction devices: FTO glasses were ultrasonically cleaned using acetone, ethanol, and deionized water, respectively. Then they were dried with nitrogen stream and cleaned by UVO light for 10 min immediately before use. The Nb doping TiO_2 (Nb/Ti = 0.05, mol/mol) layer (30-40 nm) was prepared by the chemical bath deposition method (0.2 M $TiCl_4$ aqueous solution with $NbCl_5$ hydrochloric acid (38%) solution (0.18 g/ml) at 70 °C for 76 min) according to the previous report [1].

1.5 M $Cs_xFA_{1-x}Pb(I_yBr_{1-y})_3$ perovskite precursor solution was made by dissolving different ratio of CsBr, FAI, PbI_2, and $PbBr_2$ into the mixed solvent of DMF and DMSO (Volume ratio of DMF: DMSO is 4: 1), the solution was stirred at 50 °C for 3 h till completely dissolved and filtered using

a 0.22-μm PTFE filter before use. Spin-coating plus vacuum method was applied for preparing perovskite films in glovebox, while the fabrication details can be seen in our previous repot, specifically, 50 μL of the precursor solution was dropped on TiO_2 substrates and spin-coated at 4000 rpm for 10 s, afterwards, they were transferred into a chamber connected to a rotary vane vacuum pump (vacuum capacity: 16 m^3/h), we subsequently opened the valve of the pump and the pressure of the chamber rapidly dropped, when the color of the wet film changed, the pump was closed and the chamber was rapidly purged. The substrate was subsequently transferred to a hotplate and annealed at 130°C for 15 min. The hole transporting layer (HTL) was prepared by spin coating at 4000 rpm for 30 s using a chlorobenzene solution by dissolving 90 mg spiro-OMeTAD in 1 ml chlorobenzene with the addition of 45 μl Li-TFSI/acetonitrile (170 mg/ml) and 75 μl KF209/acetonitrile (100 mg/ml), and 10 μl TBP. Finally, 100 nm of gold was prepared by thermal evaporation.

Fabrication of Tandem devices: The silicon heterojunction cells (SHJ) was fabricated as follows: An n-type, 280-μm-thick, front-side polished and rear-side textured, float-zone wafer was used as the starting substrate. The wafers were cleaned using the standard RCA process, and the resulting oxides were removed by dipping in diluted hydrofluoric acid immediately before a-Si:H deposition. The a-Si:H, doped p, and n type layers were prepared in three separate chambers of the RFPECVD system to avoid cross contamination. On the front-side of the wafer, 20-nm ITO tunnel junction layers were prepared using sputtering deposition. The back contacts were formed through sputtering of 80 nm ITO and thermal evaporation of 600 nm Al.

The perovskite top cell was then deposited onto the ITO intermediate recombination layer using the following process: The substrates were cleaned using a 20-min UV-O_3 treatment. Subsequently, SnO_2 solution (2.67%, diluted by water) was spin-coated on the substrate at 4,000 r.p.m. for 30 s, and annealed in ambient air at 150 °C for 30 min. Before it was transported into the N_2 glove box, treating with UV-O_3 for 20 min. Then 1.5 M precursor solution of the $Cs_{0.15}FA_{0.85}Pb(I_{0.8}Br_{0.2})_3$ perovskite absorber layer was fabrication on SnO_2 substrates. GuABr solution was dissolved in IPA with a concentration of 1 mg/mL and spin-coated onto the perovskite surface at a spin rate of 5000 r.p.m. for 30 s without annealing. The hole transport layer was deposited on top of the sample layer at a spin rate of 5000 r.p.m. for 30 s using spiro-OMeTAD solution, which consisted of 72.3 mg spiro-OMeTAD, 35 μL bis(trifluoromethane) sulfonimide lithium salt (LiTFSI) stock solution (260 mg LiTFSI in 1 mL acetonitrile), 30 μL 4-tertbutylpyridine and 1 mL chlorobenzene. For the front transparent electrode, 12 nm thick MoO_x buffer layer was thermally evaporated on the substrate in a vacuum chamber at a base pressure around 2×10^{-4} mbar and deposition rates of 0.1 Å/s. Then the top contact was formed by 100 nm IZO deposited using RF magnetron sputtering in a KJLC Lab-18 sputtering system at room temperature without further annealing of the sample. The square resistance was ~50 Ω/sq measured by four-point probe. The RF power during the film deposition was 40 W. Gold electrode was thermally evaporated on the top through a shadow mask

defined a frame around the transparent cell with the area of 0.5091 cm^2. Finally, a light management antireflective foils of polydimethylsiloxane (PDMS) polymer with pyramid size of 3-5 μm was put on the top of the active area.

Films and device characterization: The XRD spectra of annealed perovskite films were obtained using a D/max 2500 PC X-ray diffractometer with Cu, Ka radiation (Rigaku Corporation). The SEM images were obtained by using a field-emission scanning electron microscope (S-4800. Hitachi Corporation). The root mean square (RMS) was measured using a Contour GT noncontact three-dimensional (3D) profilometer (Bruker Corporation). The absorption spectra were measured using an UV-Vis spectrometer (UV-2600, Shimadzu Corporation). The *J-V* characteristics of photovoltaic cells were measured by a Keithley 2400 source and the solar simulator with standard AM 1.5 G (100 mW/cm^2, SSF5-3A: Enlitech). The light intensity was calibrated by applying an Si reference cell with a KG5-filter (SRC-2020-KG5-RTD, Enlitech), The *J-V* curves were measured by forward (-0.1 V to 1.5 V forward bias) or reverse (1.5 V to -0.1 V) scans; the step was 0.02 V; the delay time between steps was 50 ms. The incident photon-to-current conversion efficiency (IPCE) was measured using an EnliTech IPCE measurement system (QE-R3011, Enli Technology Co., Ltd.). An 8-degree angle integral total reflection was measured by the same system. A 3*3-mm metal mask was used for the IPCE and *J-V* measurement. Photoluminescence decay kinetics were measured using the F900 Edinburgh Instruments time-correlated single photon counting fluorescence spectrometer. Semiconductor diode laser EPL-470 emitting 72 ps pulses at 470 nm was utilized in transient measurements for sample excitation. The pulse repetition rate was 500 kHz (2μs) and the time resolution of the setup was about several hundreds of picoseconds by applying apparatus function deconvolution.

For the characterization for tandem devices, *J-V* curves of solar cells were measured at 25 °C under the AM 1.5G (100 mW/cm^2) illumination. Unless specified, bias scan from 2.0 V to 0 V firstly (reverse scan) and return back (forward scan) with a voltage step of 40 mV and delay time 0.05 s. The spectral response was taken by external quantum efficiency (EQE) measurement system (QEX10, PV Measurement) in the wavelength from 300 to 1200 nm with a scanning step of 10 nm. Xenon arc lamp was used as the monochromatic light excitation source and filtered by a double grating. The frequency of monochromatic light was around 80 Hz. Each individual sub-cell in the tandem must be electrically isolated to obtain an EQE spectrum. The top cell was measured by saturating the bottom cell with infrared light (> 800 nm), whereas the bottom cell was measured by saturating the top cell with blue light (400-500 nm).
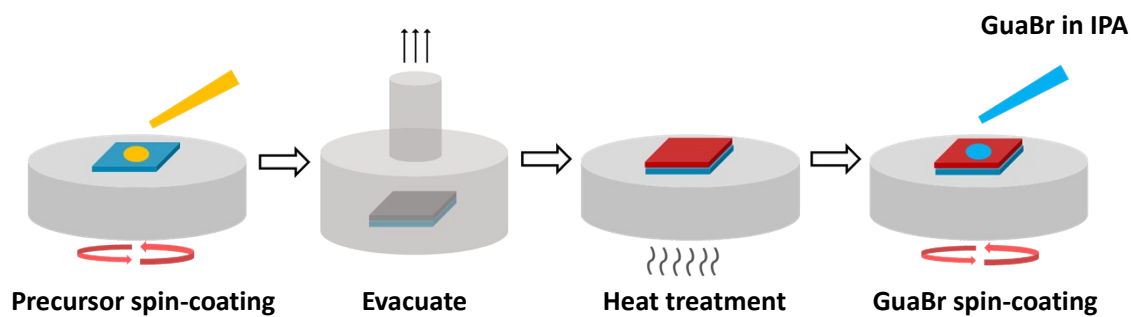
Fig. S1. Schematic illustration depicting the fabrication process of perovskite films passivated with GuaBr.
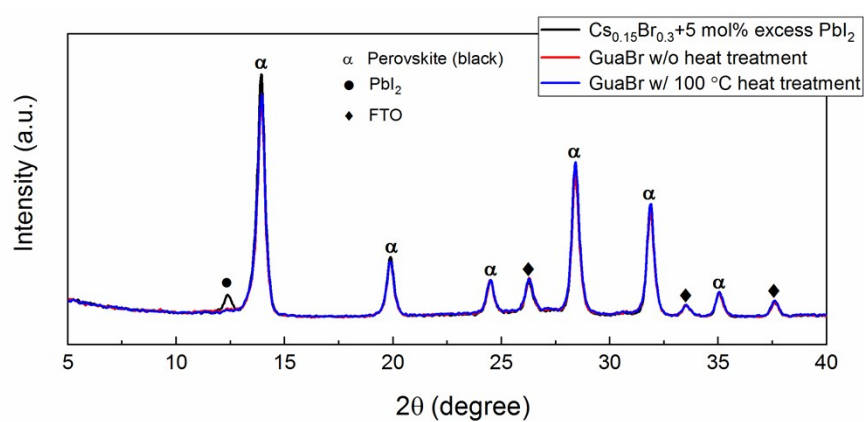

Fig. S2. XRD patterns of as-prepared perovskite films containing an initial amount of PbI_2 excess before and after GuaBr passivation.
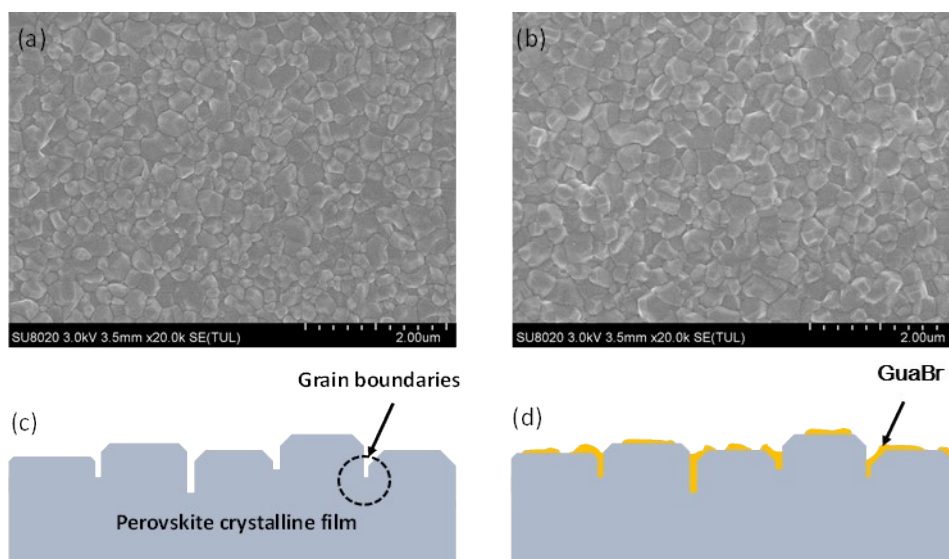
Fig. S3. Surface SEM images of as-prepared perovskite films (a) and GuaBr treated perovskite films (b). (c-d) Schematic diagram showing the proposed change of cross sectional structures after GuaBr coating.

Samples	V_{oc} (V)	J_{sc} (mA/cm^2)	FF (%)	PCE (%)
$Cs_{0.15}Br_{0.3}$	1.188	19.96	76.9	18.23
1 mg	1.209	20.24	80.4	19.67
3 mg	1.232	19.91	77.1	18.91
5 mg	1.233	19.72	76.9	18.70
7 mg	1.234	19.43	75.0	17.99
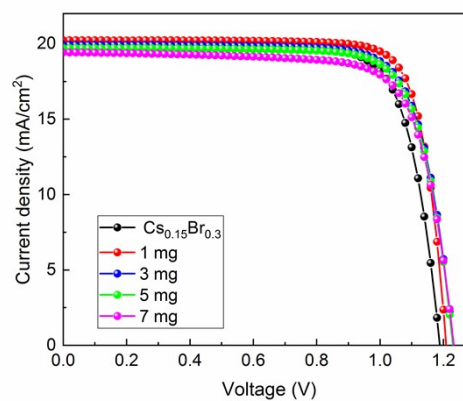
Fig. S4. *J-V* curves of PSCs employing different concentration of GuaBr.
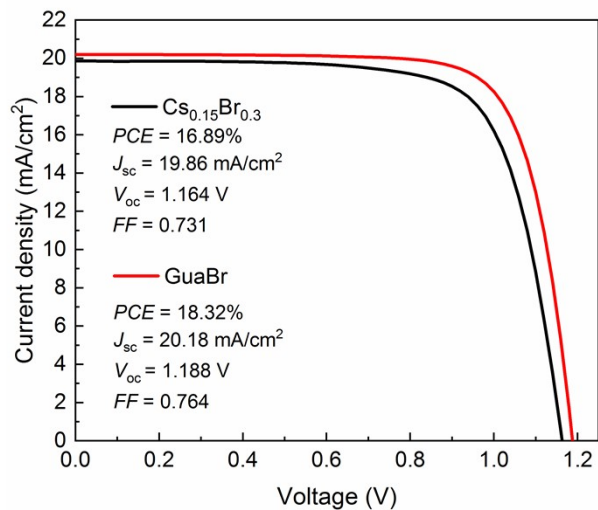
Fig. S5. *J-V* curves of the champion cells based on $Cs_{0.15}Br_{0.3}$ with and without GuaBr under forward scan.
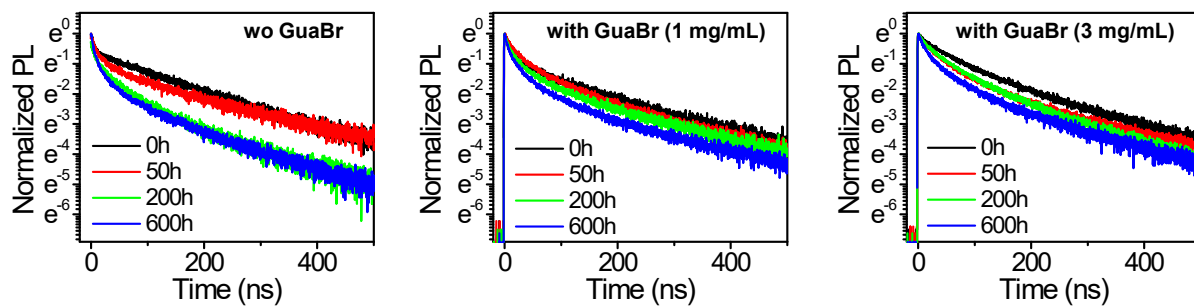
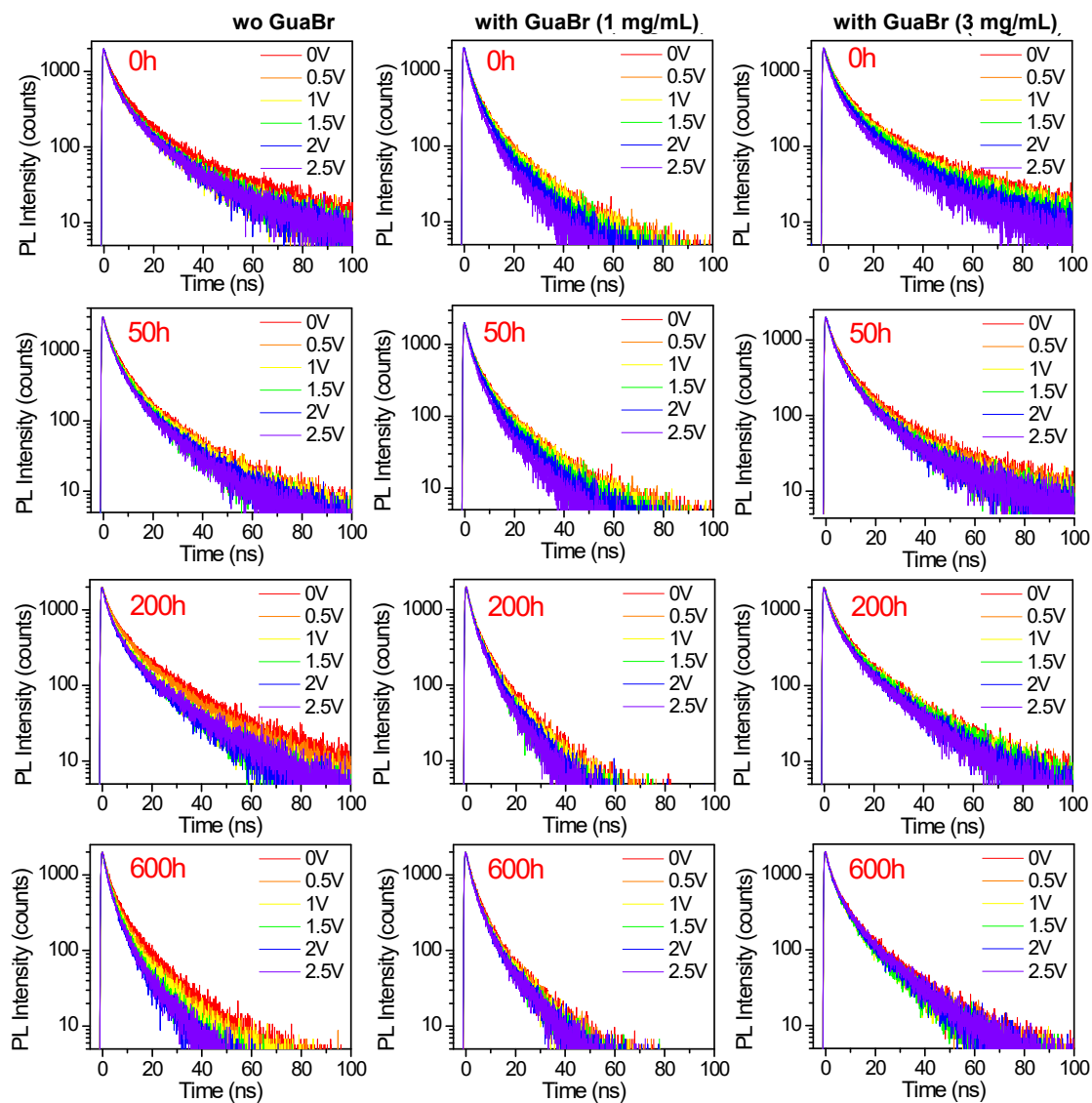**Fig. S6**. Photoluminescence decay kinetics of the pristine and GuaBr treated Cs_xBr_{1-y} perovskite films obtained at different aging times.

Table S1. Summary of the fitting parameters for the PL decay kinetics of the pristine and GuaBr treated Cs_xBr_{1-y} perovskite films.

Time, h	Sample	A1, %	$\tau 1$, ns	A2, %	$\tau 2$, ns
0 h	Ref	46.8	5.7	53.2	153.9
0 h	1mg/mL	58.5	9.7	41.5	152.1
0 h	3mg/mL	46.0	40.5	54.0	158.9
50 h	Ref	61.0	12.0	39.0	166.8
50 h	1mg/mL	58.8	20.0	41.2	135.8
50 h	3mg/mL	60.9	29.4	39.1	148.7
200 h	Ref	56.1	10.2	43.9	90.9
200 h	1mg/mL	65.3	14.9	34.7	138.0
200 h	3mg/mL	51.7	27.3	48.3	126.0
600 h	Ref	74.0	8.3	26.0	97.6
600 h	1mg/mL	70.2	12.3	29.8	135.1
600 h	3mg/mL	63.3	17.7	36.7	128.3

Fig. S7. Voltage-dependent photoluminescence decay kinetics of the pristine and GuABr treated Cs_xBr_{1-y} perovskite devices obtained at different aging times under light illumination at room temperature conditions.
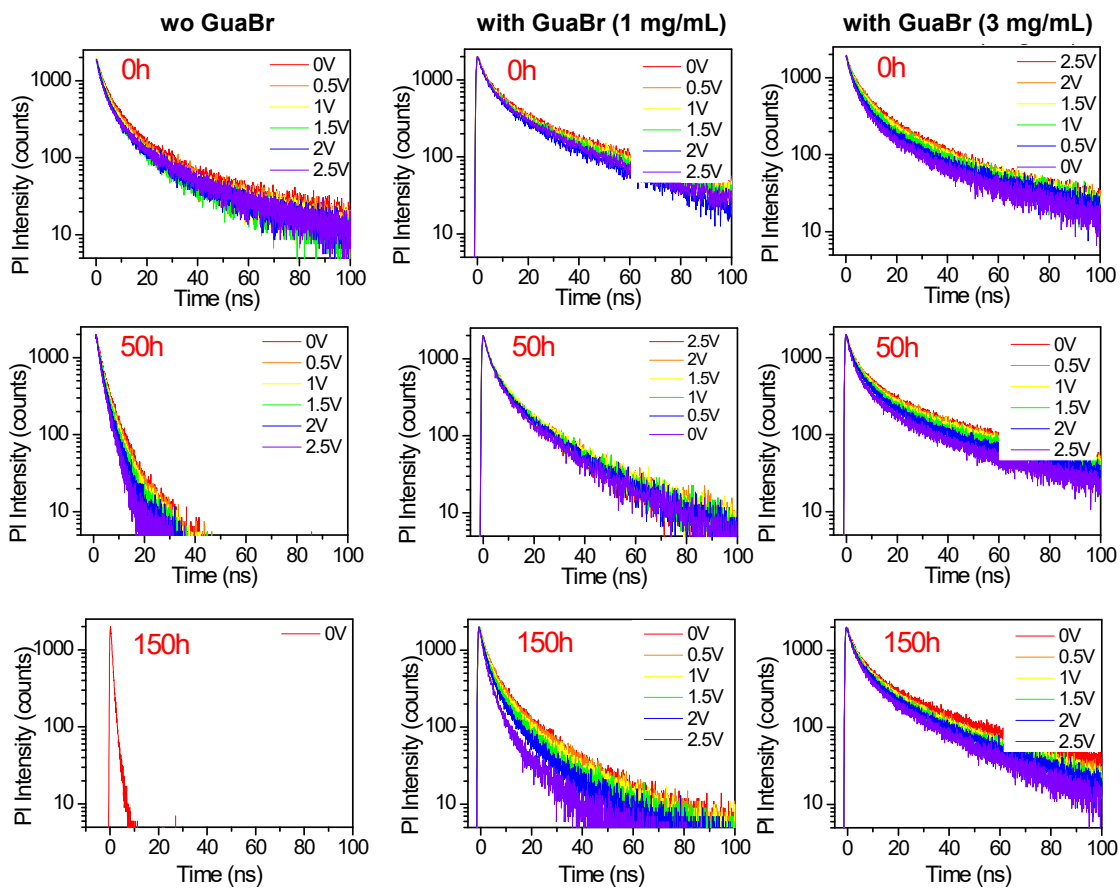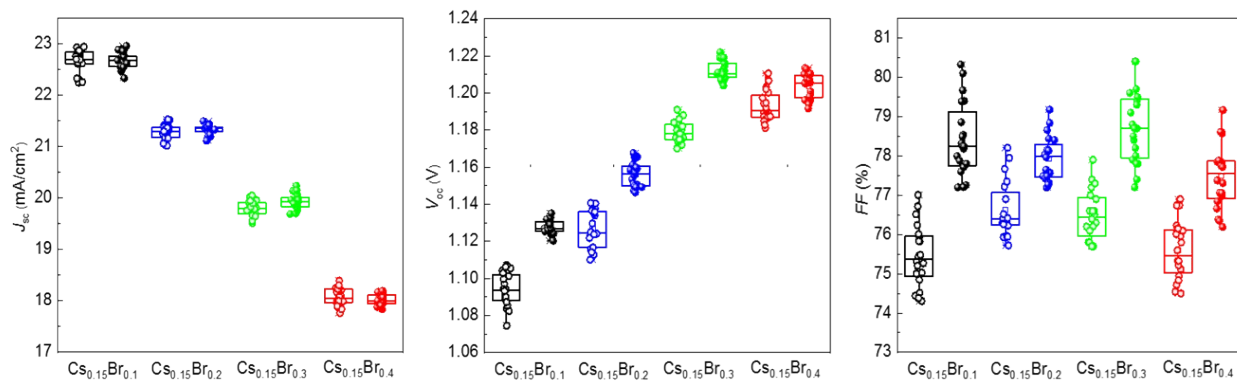
Fig. S8. Voltage-dependent photoluminescence decay kinetics of the pristine and GuaBr treated Cs_xBr_{1-y} perovskite devices obtained at different aging times under light illumination at 85°C temperature conditions.

Fig. S9. Statistical analysis of the photovoltaic parameters obtained for $Cs_{0.15}FA_{0.85}Pb(I_yBr_{1-y})_3$ cells presented in Table S1, with (filled symbols) and without (open symbols) GuaBr treatment.
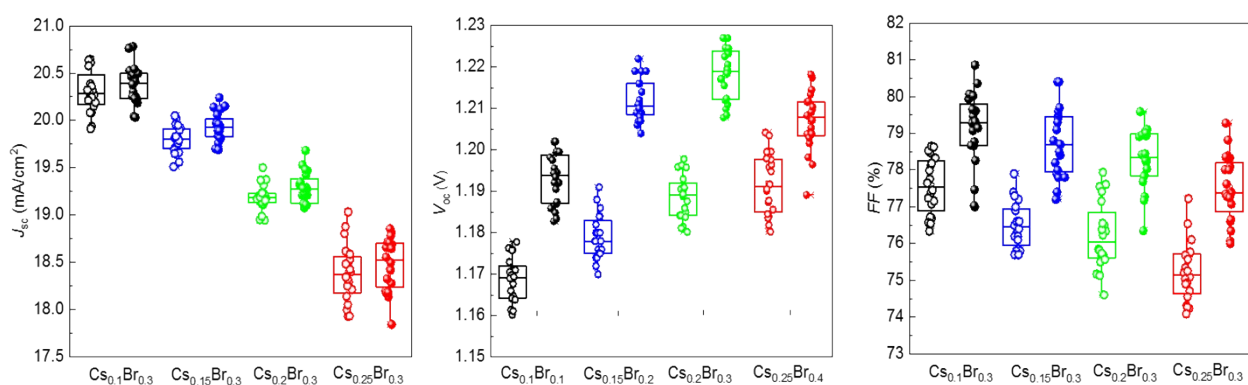
Fig. S10. Statistical analysis of the photovoltaic parameters obtained for $Cs_xFA_{1-x}Pb(I_{0.7}Br_{0.3})_3$ cells presented in Table S2, with (filled symbols) and without (open symbols) GuaBr treatment.

Table S2. Photovoltaic performance of cells prepared with $Cs_{0.15}FA_{0.85}Pb(I_y Br_{1-y})_3$ and varying y values.

Samples		V_{oc} (V)	J_{sc} (mA/cm²)	FF (%)	PCE (%)
y=0.9	(average)	1.094	22.67	75.5	18.71
	(Champion)	1.103	22.70	76.5	19.16
y=0.9+GuABr	(average)	1.128	22.67	78.4	20.05
	(Champion)	1.129	22.54	80.1	20.39
y=0.8	(average)	1.127	21.28	76.6	18.37
	(Champion)	1.136	21.30	78.2	18.92
y=0.8+GuABr	(average)	1.156	21.34	77.9	19.22
	(Champion)	1.159	21.32	78.8	19.49
y=0.7	(average)	1.179	19.80	76.5	17.86
	(Champion)	1.188	19.96	76.9	18.23
y=0.7+GuABr	(average)	1.212	19.93	78.7	19.02
	(Champion)	1.209	20.24	80.4	19.67
y=0.6	(average)	1.193	18.08	75.6	16.30
	(Champion)	1.203	18.39	75.3	16.67
y=0.6+GuABr	(average)	1.204	18.02	77.5	16.81
	(Champion)	1.201	17.99	79.2	17.10

Table S3. Photovoltaic performance of cells prepared with $Cs_xFA_{1-x}Pb(I_{0.7}Br_{0.3})_3$ and varying x values.

Samples		V_{oc} (V)	J_{sc} (mA/cm^2)	FF (%)	PCE (%)
x=0.1	(average)	1.169	20.31	77.6	18.41
	(Champion)	1.176	20.36	78.6	18.83
x=0.1+GuaBr	(average)	1.193	20.38	79.1	19.23
	(Champion)	1.202	20.78	79.1	19.75
x=0.15	(average)	1.179	19.80	76.5	17.86
	(Champion)	1.188	19.96	76.9	18.23
x=0.15+GuaBr	(average)	1.212	19.93	78.7	19.02
	(Champion)	1.209	20.24	80.4	19.67
x=0.2	(average)	1.189	19.19	76.2	17.38
	(Champion)	1.198	19.50	76.6	17.88
x=0.2+GuaBr	(average)	1.218	19.28	78.3	18.40
	(Champion)	1.225	19.47	79.1	18.86
x=0.25	(average)	1.192	18.39	75.2	16.48
	(Champion)	1.203	19.03	75.6	17.31
y=0.25+GuaBr	(average)	1.207	18.48	77.5	17.29
	(Champion)	1.218	18.85	77.2	17.74

Table S4. Photovoltaic performance of Si/perovskite tandem cells.

	V_{oc} (V)	J_{sc} (mA/cm^2)	FF (%)	PCE (%)
Control-Forward	1.858	17.70	69.74	22.93
Control-Reverse	1.839	17.75	62.14	20.29
Control-Average	1.831	16.52	66.58	19.72
GuaBr-Forward	1.915	17.33	72.33	24.01
GuaBr-Reverse	1.885	17.39	64.78	21.23
GuaBr-Average	1.895	16.16	69.72	21.89
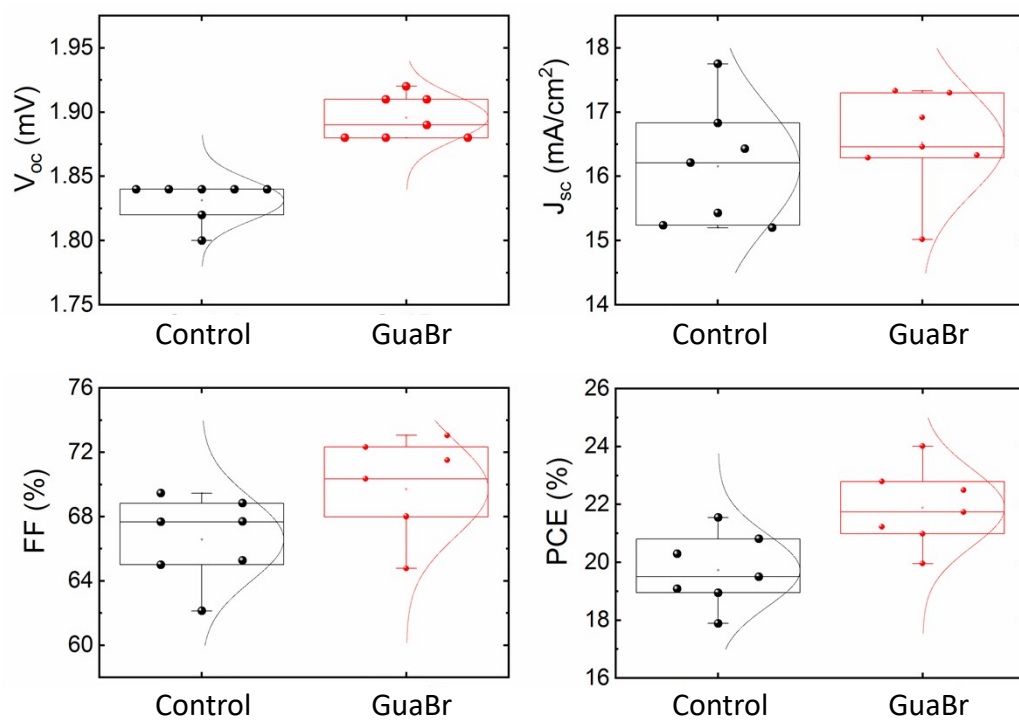
Fig. S11. Statistical analysis of the photovoltaic parameters obtained for the Si/perovskite tandem cells.

Table S5. Summary of 2 terminal perovskite (n-i-p structure)/ Silicon tandem solar cells reported so far.

V_{oc} (V)	J_{sc} (mA/cm^2)	FF (%)	PCE (%)	Ref
1.58	11.5	75.0	13.7	2
1.64	15.3	64.8	16.3	3
1.71	15.5	71.0	18.8	4
1.79	14.0	79.5	19.9	5
1.70	15.3	79.2	20.6	6
1.68	16.1	78.0	21.0	7
1.65	16.1	79.9	21.2	8
1.83	16.7	70.0	21.3	9
1.69	15.8	79.9	21.4	10
1.84	15.2	77.3	21.6	11
1.74	16.2	78.0	21.9	12
1.75	16.9	74.2	21.9	13
1.66	16.5	81.1	22.2	14
1.75	16.8	77.1	22.7	15
1.75	17.6	73.8	22.8	16
1.73	16.5	81.0	23.1	17
1.78	17.8	75.0	23.7	18
1.76	17.8	78.1	24.5	19
1.92	17.3	72.3	24.0	This work

Table S6. Summary of n-i-p type single junction perovskite solar cells ($E_g \geq 1.63$ eV and PCE > 15%)

Perovskite	PCE (%)	V_{OC} (V)	J_{SC} (mA/cm^2)	FF (%)	Eg (eV)	Ref.
$Rb_{0.05}(FA_{0.75}MA_{0.15}Cs_{0.1})_{0.95}PbI_2Br$	15.90	1.12	19.40	73.0	1.73	[20]
$FA_{0.83}Cs_{0.17}Pb(I_{0.6}Br_{0.4})_3$	16.28	1.16	18.27	78.5	1.75	[21]
$FA_{0.85}Cs_{0.15}Pb(I_{0.73}Br_{0.27})_3$	18.13	1.24	19.83	73.7	1.72	[22]
$FA_{0.8}Cs_{0.2}Pb(I_{0.7}Br_{0.3})_3$	18.27	1.25	18.53	79.0	1.75	[23]
$FA_{0.17}Cs_{0.83}PbI_{2.2}Br_{0.8}$	18.60	1.24	19.80	75.0	1.72	[24]
$K_{0.1}(Cs_{0.06}FA_{0.79}MA_{0.15})_{0.9}Pb(I_{0.4}Br_{0.6})_3$	17.50	1.23	17.90	79.0	1.78	[25]
$FA_{0.83}Cs_{0.17}Pb(I_{0.6}Br_{0.4})_3$	17.80	1.23	18.34	79.0	1.75	[26]
$Cs_{0.17}FA_{0.83}PbI_{2.2}Br_{0.8}$	18.60	1.27	19.30	77.4	1.72	[27]
$Cs_{0.12}MA_{0.05}FA_{0.83}Pb(I_{0.6}Br_{0.4})_3$	19.10	1.25	19.00	81.5	1.74	[28]
$Rb_5(Cs_5MAFA)_{95}Pb(I_{0.83}Br_{0.17})_3$	21.60	1.24	22.80	81.0	1.63	[29]
$FA_{0.83}Cs_{0.17}Pb(I_{0.6}Br_{0.4})_3$	17.00	1.20	19.40	75.1	1.74	[30]
$Cs_{0.2}FA_{0.8}Pb(I_{0.75}Br_{0.25})_3$	20.70	1.22	21.20	80.5	1.65	[31]
$BA_{0.09}(FA_{0.83}Cs_{0.17})_{0.91}Pb(I_{0.6}Br_{0.4})_3$	17.30	1.18	19.80	73.0	1.72	[32]
$FA_{0.15}Cs_{0.85}Pb(I_{0.73}Br_{0.27})_3$	18.10	1.24	19.83	73.7	1.72	[33]
$FA_{0.83}Cs_{0.17}Pb(I_{0.6}Br_{0.4})_3$	19.50	1.31	19.30	78.0	1.72	[34]
$Rb_{0.05}Cs_{0.095} MA_{0.1425} FA_{0.7125}PbI_2Br$	17.10	1.21	18.00	78.9	1.72	[28]
$Cs_{0.25}FA_{0.75}Pb(I_{0.8}Br_{0.2})_3$	20.04	1.13	21.69	82.0	1.65	[25]

$Cs_{0.05}MA_{0.15}FA_{0.8}Pb(I_{0.75}Br_{0.25})_3$	19.80	1.20	21.60	76.6	1.68	[26]
$FA_{0.83}Cs_{0.17}Pb(I_{0.80}Br_{0.20})_3$	19.24	1.22	20.38	77.2	1.68	[27]
$Cs_{0.15}FA_{0.85}Pb(I_{0.7}Br_{0.3})_3$	**19.67**	**1.21**	**20.24**	**80.4**	**~1.7**	**This work**

References

[1] Duong T, Wu Y L, Shen H P, Peng J, Fu X, Jacobs D, Wang E-C, Kho T C, Fong K C, Stocks M, Franklin E, Blakers A, Zin N, McIntosh K, Li W, Cheng Y B, White T P, Weber K, Catchpole K, 2017 Adv. Energy Mater. 7 1700228.

[2] Yang M J, Kim D H, Yu Y, Li Z, Reid O G, Song Z N, Zhao D W, Wang C L, Li L W, Meng Y, Guo T, Yan Y F, Zhu K, 2018 Mater. Today. Energy 7 232.

[3] Zhou Y, Wang F, Cao Y, Wang J P, Fang H H, Loi M A, Zhao N, Wong C P, 2017 Adv. Energy Mater. 7 1701048.

[4] Yu Y, Wang C L, Grice C R, Shrestha N, Zhao D W, Liao W Q, Guan L, Awni R A, Meng W W, Cimaroli A J, Zhu K, Ellingson R J, Yan Y F, 2017 ACS Energy Lett. 2 1177.

[5] Zhou Y, Jia Y H, Fang H H, Loi M A, Xie F Y, Gong L, Qin M C, Lu X H, Wong C P, Zhao N, 2018 Adv. Funct. Mater. 28 1803130.

[6] Abdi-Jalebi M, Andaji-Garmaroudi Z, Cacovich S, Stavrakas C, Philippe B, Richter J M, Alsari M, Booker E P, Hutter E M, Pearson A J, Lilliu S, Savenije T J,Rensmo H, Divitini G, Ducati C, Friend R H, Stranks S D, 2018 Nature 555 497.

[7] Kim J, Saidaminov M I, Tan H R, Zhao Y C, Kim Y, Choi J, Jo J W, Fan J, Quintero‑Bermudez R, Yang Z Y, Quan L N, Wei M Y, Voznyy O, Sargent E H, 2018 Adv. Mater. 30 1706275.

[8] Duong T, Pham H, Kho T H, Phang P, Fong, K C, Yan D, Yin Y T, P J, Mahmud M A, Gharibzadeh S, Nejand B A, Hossain I M, Khan M R, Mozaffari N, Wu Y L, Shen H P, Zheng J H, Mai H X, Liang W S, Samundsett C, Stocks M, McIntosh K, Andersson G G, Lemmer U, Richards B S, Paetzold U W, Ho-Ballie A, Liu Y, Macdonald D, Blakers A, Wong-Leung J, White T, Weber K, Catchpole K, 2019 Adv. Energy Mater. 10 1903553.

[9] Tan H R, Che F L, Wei M Y, Zhao Y C, Saidaminov M I, Petar T, Danny B, Grant W, Tan F R, Zhuang T T, 2018 Nat. Commun. 9 3100.

[10] Saliba M, Matsui T, Domanski K, Seo J Y, Ummadisingu A, Zakeeruddin S M, Correa-Baena J P, Tress W R, Abate A, Hagfeldt A, Grätzel M, 2016 Science 354 206.

[11] McMeekin D P, Sadoughi G, Rehman W, Eperon G E, Saliba M, Hörantner M T, Haghighirad A, Sakai N, Korte L, Rech B, Johnston M B, Herz L M, Snaith H J, 2016 Science 351 151.

[12]Wang Z P, Lin Q Q, Chmiel F P, Sakai N, Herz L M, Snaith H J, 2017 Nat. Energy 2 17135.

[13] Zhuang J, Mao P, Luan Y G, Yi X H, Tu Z Y, Zhang Y Y, Yi Y P, Wei Y Z, Chen N L, Lin T, Wang F Y, Li C, Wang J Z, 2019 ACS Energy Lett. 4 2913.

[14] Gharibzadeh S, Abdollahi Nejand B, Jakoby M, Abzieher T, Hauschild D, Moghadamzadeh S, Schwenzer J A, Brenner P, Schmager R, Haghighirad A A, Weinhardt L, Lemmer U, Richards B S, Howard I A, Paetzold U W, 2019 Adv. Energy Mater. 9 1803699.

[15] X. Wang, Y. Chen, T. Zhang, X. Wang, Y. Wang, M. Kan, Y. Miao, H. Chen, X. Liu, X. Wang, J. Shi, L. Zhang, Y. Zhao, ACS Energy Lett. 2021, 6, 2735−2741.

[16] E. Aydin, J. Liu, E. Ugur, R. Azmi, G. T. Harrison, Y. Hou, B. Chen, S. Zhumagali, M. De Bastiani, M. Wang, W. Raja, T. G. Allen, A. ur Rehman, A. S. Subbiah, M. Babics, A. Babayigit, F. H. Isikgor, K. Wang, E. V. Kerschaver, L. Tsetseris, E. H. Sargent, F. Laquai, S. D. Wolf, Energy Environ. Sci., 2021, DOI:10.1039/D1EE01206A.

[17] B. Chen, P. Wang, R. Li, N. Ren, Y. Chen, W. Han, L. Yan, Q. Huang, D. Zhang, Y. Zhao, X. Zhang, J. Energy Chem., 2021, DOI:10.1016/j.jechem.2021.07.018.

[18] J.P. Mailoa, C.D. Bailie, E.C. Johlin, E.T. Hoke, A.J. Akey, W.H. Nguyen, M.D. McGehee, T. Buonassisi, Appl. Phys. Lett. 106 (2015) 121105.

[19] A. Al-Ashouri, E. Köhnen, B. Li, A. Magomedov, H. Hempel, P. Caprioglio, J.A. Márquez, A.B.M. Vilches, E. Kasparavicius, J.A. Smith, N. Phung, D. Menzel, M. Grischek1, L. Kegelmann, D. Skroblin, C. Gollwitzer, T. Malinauskas, M. Jošt, G. Matic, B. Rech, R. Schlatmann, M. Topic, L. Korte, A. Abate, B. Stannowski, D. Neher, M. Stolterfoht, T. Unold, V. Getautis, S. Albrecht, Sicence 370 (2020) 1300-1309.

[20] J. Werner, A. Walter, E. Rucavado, S.-J. Moon, D. Sacchetto, M. Rienaecker, R. Peibst, R. Brendel, X. Niquille, S. De Wolf, P. Löper, M. Morales-Masis, S. Nicolay, B. Niesen, C. Ballif, Appl. Phys. Lett. 109 (2016) 233902.

[21] S. Zhu, X. Yao, Q. Ren, C. Zheng, S. Li, Y. Tong, B. Shi, S. Guo, L. Fan, H. Ren, C. Wei, B. Li, Y. Ding, Q. Huang, Y. Li, Y. Zhao, X. Zhang, Nano Energy. 45 (2018) 280-286.

[22] S. Albrecht, M. Saliba, J. P. C. Baena, F. Lang, L. Kegelmann, M. Mews, L. Steier, A. Abate, J. Rappich, L. Korte, R. Schlatmann, M.K. Nazeeruddin, A. Hagfeldt, M. Gratzeld, B. Rech, Energy Environ. Sci. 9 (2016) 81.

[23] R. Fan, N. Zhou, L. Zhang, R. Yang, Y. Meng, L. Li, T. Guo, Y. Chen, Z. Xu, G. Zheng, Y. Huang, L. Li, L. Qin, X. Qiu, Q. Chen, H. Zhou, Solar RRL 1 (2017) 1700149.

[24] J. Zheng, C.F.J. Lau, H. Mehrvarz, F.-J. Ma, Y. Jiang, X. Deng, A. Soeriyadi, J. Kim, M. Zhang, L. Hu, X. Cui, D.S. Lee, J. Bing, Y. Cho, C. Chen, M.A. Green, S. Huang, A.W.Y. Ho-Baillie, Energy Environ. Sci. 11 (2018) 2432-2443.

[25] C.U. Kim, J.C. Yu, E.D. Jung, I.Y. Choi, W. Park, H. Lee, I. Kim, D.-K. Lee, K.K. Hong, M.H. Song, K.J. Choi, Nano Energy 60 (2019) 213-221.

[26] J. Werner, C.H. Weng, A. Walter, L. Fesquet, J.P. Seif, S. De Wolf, B. Niesen, C. Ballif, J. Phys. Chem. Lett. 7 (2016) 161-166.

[27] F. Hou, L. Yan, B. Shi, J. Chen, S. Zhu, Q. Ren, S. An, Z. Zhou, H. Ren, C. Wei, Q. Huang, G. Hou, X. Chen, Y. Li, Y. Ding, G. Wang, D. Zhang, Y. Zhao, X. Zhang, ACS Appl. Energy Mater. 2 (2019) 243-249.

[28] A.J. Bett, P.S.C. Schulze, K.M. Winkler, Ö.S. Kabakli, I. Ketterer, L.E. Mundt, S.K. Reichmuth, G. Siefer, L. Cojocaru, L. Tutsch, M. Bivour, M. Hermle, S.W. Glunz, J.C. Goldschmidt, Prog Photovolt. 28 (2019) 99-110.

[29] J. Zheng, H. Mehrvarz, F.-J. Ma, C.F.J. Lau, M.A. Green, S. Huang, A.W.Y. Ho-Baillie, ACS Energy Lett. 3 (2018) 2299-2300.

[30] F. Hou, C. Han, O. Isabella, L. Yan, B. Shi, J. Chen, S. An, Z. Zhou, W. Huang, H. Ren, Q. Huang, G. Hou, X. Chen, Y. Li, Y. Ding, G. Wang, C. Wei, D. Zhang, M. Zeman, Y. Zhao, X. Zhang, Nano Energy 56 (2019) 234-240.

[31] Z. Qiu, Z. Xu, N. Li, N. Zhou, Y. Chen, X. Wan, J. Liu, N. Li, X. Hao, P. Bi, Q. Chen, B. Cao, H. Zhou, Nano Energy 53 (2018) 798-807.

[32] F. Sahli, B.A. Kamino, J. Werner, M. Bräuninger, B. Paviet-Salomon, L. Barraud, R. Monnard, J.P. Seif, A. Tomasi, Q. Jeangros, A. Hessler-Wyser, S. De Wolf, M. Despeisse, S. Nicolay, B. Niesen, C. Ballif, Adv. Energy Mater. 8 (2018) 1701609.

[33] J. Zheng, H. Mehrvarz, C. Liao, J. Bing, X. Cui, Y. Li, V.R. Gonçales, C.F.J. Lau, D.S. Lee, Y. Li, M. Zhang, J. Kim, Y. Cho, L.G. Caro, S. Tang, C. Chen, S. Huang, A.W.Y. Ho-Baillie, ACS Energy Lett. 4 (2019) 2623-2631.

[34] S. Zhu, F. Hou, W. Huang, X. Yao, B. Shi, Q. Ren, J. Chen, L. Yan, S. An, Z. Zhou, H. Ren, C. Wei, Q. Huang, Y. Li, G. Hou, X. Chen, Y. Ding, G. Wang, B. Li, Y. Zhao, X. Zhang, Solar RRL 2 (2018) 1800176.